decanuclear cluster.) The flow of CO + H_2 was maintained while the reactor was cooled to room temperature. The resultant bright pinkish brown solids were removed from the sealed reactor tubes in the drybox. Extraction of the solids was carried out with a 10-fold excess of [PPN][Cl] or [Et_4N][Cl] in reagent acetone (100 mL each). Deep reddish brown solutions formed immediately, but agitation of the suspensions under N_2 was continued for at least 1 h. After filtration, the solvent was evaporated to give a solution volume of 5-10 mL, and 2-propanol was added dropwise to precipitate red microcrystals, which were recovered by filtration and washed with several volumes of deionized water. The red $[PPN]_2[Os_{10}C(CO)_{24}]$ prepared in this manner exhibited an infrared spectrum with ν_{CO} = 2036 (s) and 1990 (s) cm^{-1}.

Altenatively, the synthesis was carried out in an autoclave. One gram of the material prepared by impregnation of MgO with H_2OsCl_6 was placed inside a 100-mL autoclave, which was purged with CO + H_2 (equimolar) at 1 atm and sealed. The autoclave was heated to 300 °C, held for 5 h, and then cooled to room temperature. The material was removed from the reactor in the drybox and extracted with [PPN][Cl] in acetone to yield pure $[Os_{10}C(CO)_{24}]^{2-}$. The identification was verified by infrared spectroscopy.

Acknowledgments. We thank A. L. Rheingold of the University of Delaware for the X-ray diffraction and J. Lazar of E. I. du Pont de Nemours and Co. for the mass spectrometry. The research at the University of Delaware was supported by the National Science Foundation (Grant CBT 8605699).

Registry No. MgO, 1309-48-4; $[PNN]_2[Os_5C(CO)_{14}]$, 88567-87-7; $Os_3(CO)_{12}$, 15696-40-9; CO, 630-08-0; $[PPn]_2[Os_{10}C(CO)_{24}]$, 75117-74-7; $[H_4Os_4(CO)_{12}]$, 12375-04-1.

Intermediates in the Time-Resolved and Matrix Photochemistry of (η^5-Cyclopentadienyl)rhodium Complexes: Roles of Alkane Activation and Rhodium-Rhodium Bond Formation

Simon T. Belt,[1a] Friedrich-Wilhelm Grevels,[1b] Werner E. Klotzbücher,[1b] Andrew McCamley,[1a] and Robin N. Perutz*,[1a]

Contribution from the Department of Chemistry, University of York, York YO1 5DD, UK, and Max-Planck Institut für Strahlenchemie, D-4330 Mülheim an der Ruhr, FRG.
Received March 24, 1989

Abstract: Pulsed laser photolysis studies of solutions of $Cp_2Rh_2(CO)_3$, $CpRh(CO)_2$, and $CpRh(C_2H_4)CO$ (Cp = η^5-C_5H_5) are reported using UV/vis and IR detection. The identification of the transients is supported by earlier studies of $Cp_2Rh_2(CO)_3$ in hydrocarbon glasses, by prior matrix studies of $CpRh(CO)_2$ and $CpRh(CO)(C_2H_4)$, and by matrix isolation experiments on $Cp_2Rh_2(CO)_3$ reported here. Matrix photolysis (20 K, Ar, N_2, CH_4, and CO matrices) of $Cp_2Rh_2(CO)_3$ generates $[CpRh(\mu\text{-}CO)]_2$ reversibly. Isotopic labeling and polarized photolysis demonstrates that the $Rh_2(CO)_2$ unit is planar with CO bridges perpendicular to the RhRh axis. Metal-metal bond fission of $Cp_2Rh_2(CO)_3$ is observed only in CO-doped matrices. The major photoproduct of $Cp_2Rh_2(CO)_3$ in solution is $[CpRh(\mu\text{-}CO)]_2$, which reacts with CO to re-form starting material with $k_2 = (1.2 \pm 0.1) \times 10^3$ dm^3 mol^{-1} s^{-1} at 292 K ($\Delta H^{\ddagger} = 22.3 \pm 2.5$ kJ mol^{-1}, $\Delta S^{\ddagger} = -110 \pm 10$ J mol^{-1} K^{-1}). The first observable product of photolysis of $CpRh(CO)_2$ in cyclohexane at room temperature is $CpRh(CO)(C_6H_{11})H$, formed by insertion of CpRhCO into the solvent C-H bonds within 400 ns. In the absence of other ligands, $CpRh(CO)(C_6H_{11})H$ decays by complex kinetics (probably by reaction with its reductive elimination product CpRhCO) to form $[CpRh(\mu\text{-}CO)]_2$ and then slowly to $Cp_2Rh_2(CO)_3$. The formation of $[CpRh(\mu\text{-}CO)]_2$ is quenched by high concentrations of other ligands (Et_3SiH, $P(OPh)_3$). The reactions with ligands exhibit saturation kinetics, from which the rate of reductive elimination of $CpRh(CO)(C_6H_{11})H$ is measured as $k_{-1} = (2.7 \pm 0.3) \times 10^3$ s^{-1}. The IR experiments show that photolysis of $CpRh(C_2H_4)CO$ gives a higher yield of $CpRh(CO)(C_6H_{11})H$ than that from $CpRh(CO)_2$. These experiments show that matrix isolation and room-temperature photolysis experiments are fully consistent, that the kinetics of formation of CpRh(CO)(alkyl)H are favorable, but that this C-H activation product is exceptionally unstable with respect to formation of other products via reductive elimination of alkane.

The ability of some complexes of general formula (η^5-C_5R_5)ML_2 and (η^5-C_5R_5)$ML(H)_2$ (M = Rh, Ir; R = Me, H; L = CO, PMe_3, C_2H_4) to yield products derived from insertion into the C-H bonds of unactivated alkanes and arenes has generated much excitement among organometallic chemists.[2] There is considerable evidence to indicate that these reactions proceed via intermediates of the type (η^5-C_5R_5)ML. However, not all of the intermediates produced by photolysis of the parent complexes are capable of carrying out C-H activation reactions. The nature of the balance required between the electronic and steric properties of the C_5R_5 and L groups and the metal is not yet fully understood.

The photochemistry of $CpRh(CO)_2$, $CpRh(C_2H_4)CO$ (Cp = η^5-C_5H_5), and related complexes has been investigated previously both in solution and in low-temperature matrices (Charts I and II).[3-9]

(1) (a) University of York. (b) Max-Planck Institut für Strahlenchemie.
(2) (a) Jones, W. D.; Feher, F. J. *J. Am. Chem. Soc.* **1984**, *106*, 1650. (b) Janowicz, A. H.; Bergman, R. G. *J. Am. Chem. Soc.* **1983**, *105*, 3929. (c) Periana, R. A.; Bergman, R. G. *J. Am. Chem. Soc.* **1986**, *108*, 7332. (d) Hoyano, J. K.; McMaster, A. D.; Graham, W. A. G. *J. Am. Chem. Soc.* **1983**, *105*, 7190.

(3) (a) Haddleton, D. M.; McCamley, A.; Perutz, R. N. *J. Am. Chem. Soc.* **1988**, *110*, 1810. (b) Haddleton, D. M. *J. Organomet. Chem.* **1986**, *311*, C21. (c) Earlier assignments[3a,5] of $CpRh(CO)(CH_3)H$ depended on the observation of ν(CO) alone. In recent experiments with $CpRh(^{13}CO)(C_2H_4)$ in methane matrices we have identified ν(Rh-H) as a broad, weak pair of bands at 2056 and 2069 cm^{-1}.
(4) (a) Mills, O. S.; Nice, J. P. *J. Organomet. Chem.* **1967**, *10*, 337. (b) Hill, R.; Knox, S. A. R. *J. Chem. Soc., Dalton Trans.* **1975**, 2622. (c) Oliver, A. J.; Graham, W. A. G. *Inorg. Chem.* **1971**, *10*, 1.
(5) Rest, A. J.; Whitwell, I.; Graham, W. A. G.; Hoyano, J. K.; McMaster, A. D. *J. Chem. Soc., Dalton Trans.* **1987**, 1181.
(6) Jones, W. D.; Feher, F. J. *Organometallics* **1983**, *2*, 562.
(7) (a) Marx, D. E.; Lees, A. J. *Inorg. Chem.* **1988**, *27*, 1121. (b) Wasserman, E. P.; Bergman, R. G.; Moore, C. B. *J. Am. Chem. Soc.* **1988**, *110*, 6076.

0002-7863/89/1511-8373$01.50/0

Chart I. Solution Photochemistry of $CpRh(CO)_2$ and $CpRh(C_2H_4)CO$

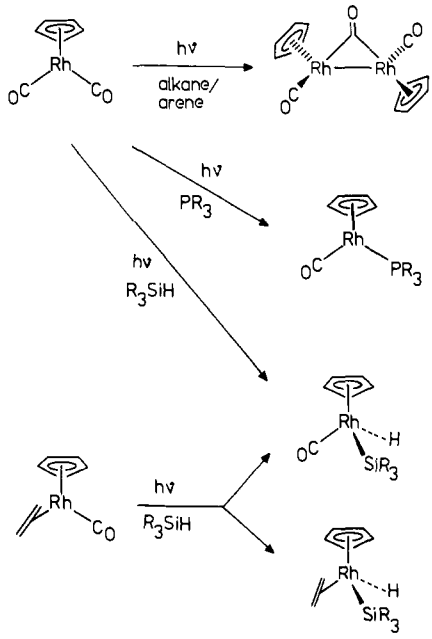

Chart II. Matrix Photochemistry of $CpRh(CO)_2$ and $CpRh(C_2H_4)CO$

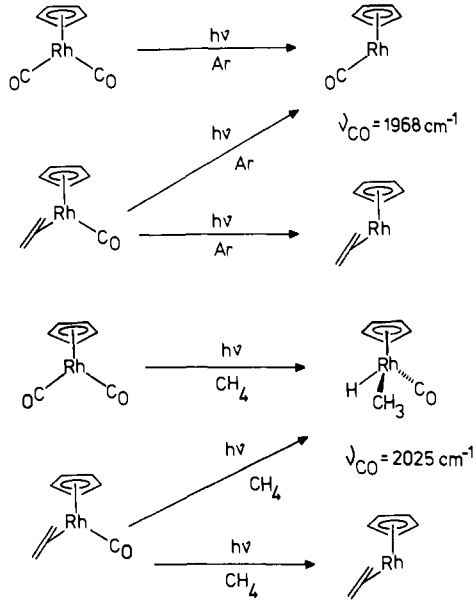

Product Studies in Solution. It has recently been shown that both the CO and C_2H_4 groups of $CpRh(C_2H_4)CO$ are photolabile,[3] while the photolability of CO in $CpRh(CO)_2$ is well established.[4] Photolysis of $CpRh(CO)_2$ in the presence of reactive substrates causes substitution (e.g., by $P(OMe)_3$)[4b] or oxidative addition (e.g., of Si–H in R_3SiH),[4c] while photolysis of $CpRh(CO)_2$ in alkane or arene solvents alone yields the dark red dinuclear complex, $Cp_2Rh_2(CO)_3$. Photolysis of $CpRh(C_2H_4)CO$ in the presence of Et_3SiH yields[3b] both $CpRh(CO)(Et_3Si)H$ and $CpRh(C_2H_4)(Et_3Si)H$. In contrast to the rhodium complexes, photolysis of $(\eta^5\text{-}C_5R_5)Ir(CO)_2$ in alkanes and arenes yields stable alkyl and aryl hydride complexes with overall loss of CO.[2d] Lees and Marx recently reported investigations[7a] of the quantum yield (φ) for the photochemical formation of (aryl) hydride complexes from $CpIr(CO)_2$, which led them to suggest that C–H activation of benzene proceeds via a hapticity change (η^5 to η^3) of the Cp ligand.

Matrix Isolation Studies. Irradiation of $CpRh(C_2H_4)CO$ in an Ar matrix at 20 K results in the formation of both $CpRh(C_2H_4)$ and CpRhCO via ejection of CO and C_2H_4, respectively.[3] Rest has shown that CpRhCO can also be formed via photolysis of $CpRh(CO)_2$ in solid Ar.[5] In both cases, CpRhCO is replaced by the C–H insertion product $CpRh(CO)(CH_3)H$ if the matrix host is changed to CH_4.[3c] In contrast, no oxidative addition reaction is observed between $CpRh(C_2H_4)$ and CH_4. The failure to characterize C–H insertion reactions with CpRhCO *in solution* seems surprising given the reaction in a CH_4 matrix and has previously been explained in terms of the extreme instability of the oxidative addition products at accessible temperatures in solution.[5] Such instability is consistent with the observation that $(\eta^5\text{-}C_5Me_5)Rh(PMe_3)(alkyl)H$ complexes decompose, via reductive elimination of free alkane, above −20 °C.[2a,6] Further strong support[8] for the dissociative mechanism of C–H activation comes from the matrix studies of $CpIr(CO)H_2$.

Studies by Time-Resolved Spectroscopy. Belt et al. investigated the photolysis of $CpRh(C_2H_4)_2$ by flash photolysis with UV and IR detection.[9] Their results provided strong support for photoelimination of ethene and specific solvation of the resulting intermediate. Wasserman et al. recently reported a mechanistic investigation into the photochemistry of $CpCo(CO)_2$ in solution and in the gas phase using time-resolved infrared (TRIR) spectroscopy.[7b] In both phases, evidence was presented for photoinduced CO loss to yield CpCoCO, which undergoes reactions with added ligands or with $CpCo(CO)_2$ at comparable rates. A solvate complex, probably $CpCo(CO)(\eta^2\text{-}C_6H_6)$ is formed in benzene.[7b] Flash photolysis of $CpIr(CO)_2$ in benzene shows that CpIr(CO)PhH is formed within 20 ns of the laser flash.[7a]

With the exception of the quantum yield measurements[7a] on $CpIr(CO)_2$, all the evidence points to a dissociative mechanism for C–H activation: the precursor loses CO or H_2 to yield the reactive 16e fragment $(C_5R_5)ML$, which subsequently inserts into the C–H bonds of alkanes and arenes. The dissociative mechanism is supported by matrix investigations, by the flash photolysis evidence, and by the kinetic evidence[2] on the formation of $Cp^*M(PMe_3)(R)H$ ($Cp^* = \eta^5\text{-}C_5Me_5$).

There is, as yet, scant experimental evidence on the molecular or electronic structure of CpML intermediates. However, both ab initio and extended Hückel calculations on the CpRhCO fragment predict that it should have a bent singlet ground state (Cp–Rh–CO, 140°) with a low lying excited triplet state.[10,11]

$Cp_2Rh_2(CO)_3$. The photochemistry of $Cp_2Rh_2(CO)_3$ in solution has not been reported, but Anderson and Wrighton have shown that it loses CO photochemically in a methylcyclohexane glass at 93 K to form $[CpRh(\mu\text{-}CO)]_2$.[12] Upon warmup, this intermediate was found to be unstable above 200 K. In contrast, photolysis of the pentamethylcyclopentadienyl analogue, $Cp^*Rh_2(CO)_3$, yields $[Cp^*Rh(\mu\text{-}CO)]_2$, which is stable at room temperature and characterized crystallographically.[13]

Goals of This Study. These results leave an apparent enigma. Is CpRhCO only capable of activating alkanes in a matrix, or do the alkyl hydrides have a transient existence in solution at room temperature? Laser flash photolysis with UV/vis and IR detection has been used recently with great success to probe the mechanisms of organometallic photoreactions. Both of these methods have proved complementary to conventional solution photochemistry (product analysis) and matrix isolation studies. The increased time resolution available with UV/vis detection has allowed the detection of extremely short-lived species,[14a] while the additional structural information available from CO-stretching modes has

(8) Bloyce, P. E.; Rest, A. J.; Whitwell, I.; Graham, W. A. G.; Holmes-Smith, R. *J. Chem. Soc., Chem. Commun.* **1988**, 846.
(9) Belt, S. T.; Haddleton, D. M.; Perutz, R. N.; Smith, B. P. H.; Dixon, A. J. *J. Chem. Soc., Chem. Commun.* **1987**, 1347.
(10) Hoffman, P.; Padmanabhan, M. *Organometallics* **1983**, *2*, 1273.
(11) Veillard, A.; Dedieu, A. *Theor. Chim. Acta* **1983**, *63*, 339.
(12) Anderson, F. R.; Wrighton, M. S. *Inorg. Chem.* **1986**, *25*, 112.
(13) (a) Plank, J.; Riedle, D.; Herrmann, W. A. *Angew. Chem., Int. Ed. Engl.* **1980**, *19*, 937. (b) Green, M.; Hankey, D. R.; Howard, J. A. K.; Louca, P.; Stone, F. G. A. *J. Chem. Soc., Chem. Commun.* **1983**, 757.
(14) (a) Simon, J. E.; Xie, X. *J. Phys. Chem.* **1986**, *90*, 6751. (b) Poliakoff, M.; Weitz, E. *Adv. Organomet. Chem.* **1986**, *25*, 277. (c) Schaffner, K.; Grevels, F. W. *J. Mol. Struct.* **1988**, *173*, 51.

Table I. CO-Stretching Bands of $Cp_2Rh_2(CO)_3$ and $[CpRh(\mu\text{-}CO)]_2$ in Matrices[a]

matrix	*trans*-$Cp_2Rh_2(CO)_3$		weak "isomer" bands[b]	$[CpRh(\mu\text{-}CO)]_2$
	$\nu(CO)_t$	$\nu(CO)_b$	$\nu(CO)_t$	$\nu(CO)_b$
Ar	1988	1844	2030	1793
N_2	1986	1840	2032	1788
CH_4	1985[c]	1831	2028, 2026	1778
mcx[d]	1981	1834	2020	1778
CO	1985	1832	2028	1781
C_6H_{12}[e]	1984	1837	2026	

[a] t, terminal; b, bridging; $\bar{\nu}$ (cm^{-1}). [b] Provisionally assigned to *cis*-$Cp_2Rh_2(CO)_3$. [c] Principal component of matrix split band. [d] From ref 12, mcx = methylcyclohexane at 77 K. [e] Cyclohexane solution at 300 K.

been exploited by using time-resolved IR spectroscopy to examine the identities of metal carbonyl fragments.[7b,14b]

In this paper we will describe a mechanistic study of the photochemistry of $CpRh(CO)_2$, $CpRh(C_2H_4)CO$, and $Cp_2Rh_2(CO)_3$ using laser flash photolysis with UV/vis and IR detection. In particular, we will show how direct measurement of the rates of reaction of C–H activation products can explain the absence of such species in conventional solution studies, which instead yield dinuclear complexes as thermodynamically preferred products. We consider first the transient and matrix photochemistry of $Cp_2Rh_2(CO)_3$, since it holds the key to interpreting the reactivity of the other two complexes. Here we include data from matrix experiments with polarized photolysis, which give significant information on the structure of $[CpRh(\mu\text{-}CO)]_2$.

Results

Matrix Photochemistry of $Cp_2Rh_2(CO)_3$. When $Cp_2Rh_2(CO)_3$ is deposited into an argon matrix at 20 K, major bands are observed at 1988 and 1844 cm^{-1} corresponding to the terminal (t) and bridging (b) CO-stretching modes of the dominant trans isomer (Table I). Very weak bands are also observed at 2052 ($CpRh(CO)_2$ impurity), 2030, and 2004 cm^{-1} (to be discussed below). In addition, a trace of free CO is present in the matrix. Irradiation of the matrix (5 min, $\lambda > 200$ nm) results in 85% loss of starting material, growth of an intense band at 1793 cm^{-1}, and growth of the band of free CO (2138 cm^{-1}). There is also a slight increase in the feature at 2030 cm^{-1}, but the other weak band at 2004 cm^{-1} is destroyed. The UV/vis spectrum of $Cp_2Rh_2(CO)_3$, measured on the same matrix, shows absorptions at 272 and 324 nm and a weak band at ~430 nm, which gives rise to the red color of this dinuclear complex. Photolysis causes bleaching of the 272-nm band, growth of a new visible absorption at 540 nm, and growth of a band at ~330 nm overlapping the precursor absorption with a shoulder at ~350 nm. The matrix acquires an intense purple color. On the basis of earlier experiments in glasses[12] and the current matrix experiments, the major photolysis product with the IR band in the region of bridging carbonyls and the UV/vis absorptions may be identified as $[CpRh(\mu\text{-}CO)]_2$.

Broad-band UV photolysis of $Cp_2Rh_2(CO)_3$ in N_2 matrices leads to very similar results (Table I). The progress of formation of $[CpRh(\mu\text{-}CO)]_2$, followed by UV/vis spectroscopy, is illustrated in Figure 1a. Subsequent irradiation into the visible band of the resulting purple matrix ($\lambda > 500$ nm, 20 min) results in ca. 20% reversal to starting material, illustrating the high reactivity of $[CpRh(\mu\text{-}CO)]_2$ toward CO. Such reversibility was not observed in earlier studies in glasses.[12] The behavior of the weak IR feature at 2032 cm^{-1} does not follow that of the 1793-cm^{-1} band of $[CpRh(\mu\text{-}CO)]_2$. On short-wavelength photolysis it increases and then declines, but increases again on long-wavelength irradiation. This product is tentatively assigned[15a] as *cis*-$Cp_2Rh_2(CO)_3$. The other weak feature at ca. 2000 cm^{-1} disappears irreversibly by short-wavelength photolysis and remains unassigned.

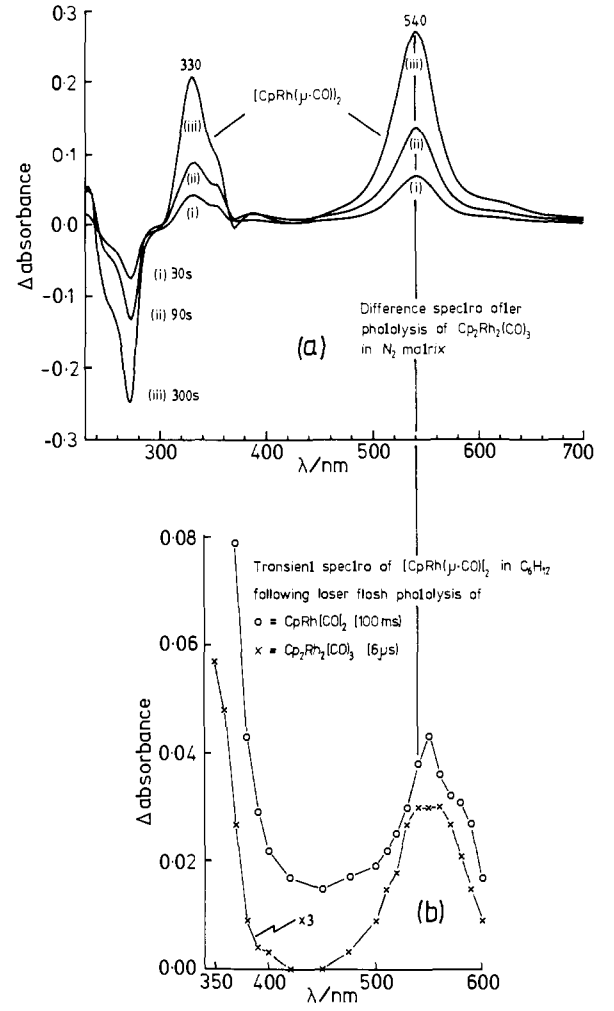

Figure 1. (a) UV/vis spectra recorded after (i) 30-, (ii) 90-, and (iii) 300-s UV photolysis ($\lambda > 200$ nm) of a nitrogen matrix at 20 K containing $Cp_2Rh_2(CO)_3$. Spectra are presented as difference spectra relative to the spectrum after deposition. Positive peaks represent growth of product $[CpRh(\mu\text{-}CO)]_2$; negative peaks represent loss of starting material. (b) Transient UV/vis spectra in cyclohexane solution at room temperature obtained (i) 6 μs after laser photolysis of $Cp_2Rh_2(CO)_3$ (×) and (ii) 100 ms after laser photolysis of $CpRh(CO)_2$ (○). In both cases the transient product is $[CpRh(\mu\text{-}CO)]_2$.

When $Cp_2Rh_2(CO)_3$ is irradiated in CO matrices (60 min, $\lambda = 314$ nm), the major product proves to be $CpRh(CO)_2$, identified by bands at 2049 and 1987 cm^{-1} (the latter overlapping the precursor), but some $[CpRh(\mu\text{-}CO)]_2$ is still formed (Table I). Further broad-band UV photolysis ($230 < \lambda < 360$ nm) increases the yield of both products. These experiments demonstrate that CO loss competes with Rh–Rh bond fission. However, Rh–Rh bond fission is suppressed by the cage effect in argon and nitrogen matrices.

Additional evidence for the stoichiometry and geometry of $[CpRh(\mu\text{-}CO)]_2$ can be obtain d by isotopic substitution. Irradiation of $Cp_2Rh_2(CO)_3$ in N_2 n .trices doped with ^{13}CO (^{13}CO:N_2 = 1:10) leads to (i) exchange of ^{13}CO with $Cp_2Rh_2(CO)_3$, (ii) formation of $CpRh(CO)_2$ and all of its ^{13}CO-labeled isotopomers, and (iii) formation of $[CpRh(\mu\text{-}CO)]_2$ and its labeled isotopomers. The initial photoproducts are slightly enriched, but enrichment increases after longer photolysis to almost 50% (Figure 2). The presence of two bands in the bridging $\nu(CO)$ region for $Cp_2Rh_2(\mu\text{-}^{12}CO)(\mu\text{-}^{13}CO)$ and one each for $[CpRh(\mu\text{-}^{12}CO)]_2$ and $[CpRh(\mu\text{-}^{13}CO)]_2$ proves that the product is a centrosymmetric bridged dicarbonyl complex. The observed and calculated frequencies, together with CO-factored force constants for $Cp_2Rh_2(CO)_3$ and $[CpRh(\mu\text{-}CO)]_2$ are given in Table II (see also Figure 2c). The force constants of $[CpRh(\mu\text{-}CO)]_2$ compare well[15b] with those for $Cp_2Fe_2(\mu\text{-}CO)_3$.

(15) (a) The related cis complex (η^5–η^5-fulvalene)$Rh_2(CO)_3$ absorbs at 2017, 1979, and 1832 cm^{-1}: Bitterwolf, T. E.; Rausch, M. D. 13th International Conference on Organometallic Chemistry, Turin, Italy, 1988; Abstract 148. (η^5–η^5-$C_5H_4CH_2C_5H_4$)$Rh_2(CO)_3$ absorbs at 2017, 1971, and 1817 cm^{-1}: Bitterwolf, T. E. *J. Organomet. Chem.* **1986**, *312*, 197. (b) Hooker, R. H.; Mahmoud, K. A.; Rest, A. J. *J. Chem. Soc., Chem., Commun.* **1983**, 1022.

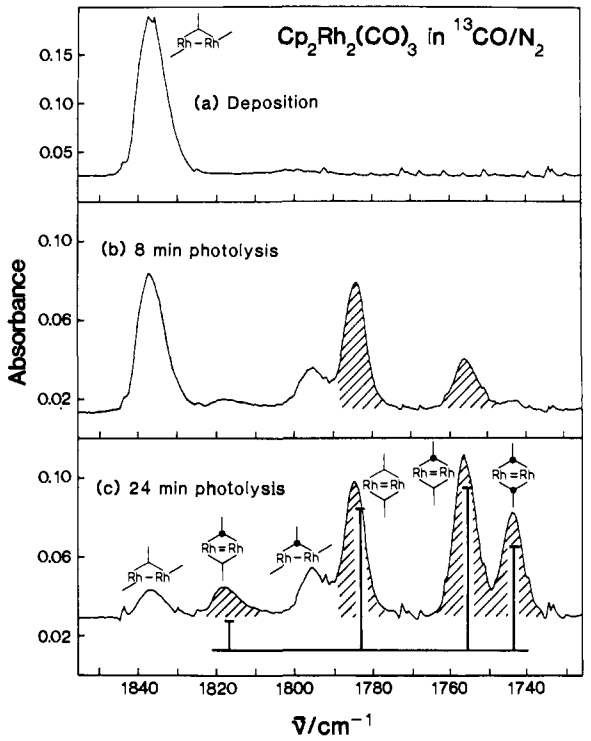

Figure 2. IR spectra in the CO-bridging region recorded on a $^{13}CO/N_2$ (1:10) matrix containing $Cp_2Rh_2(CO)_3$: (a) after deposition; (b) after 8-min photolysis with the unfiltered mercury arc; (c) after a further 24-min photolysis. Bands of $[CpRh(\mu\text{-}CO)]_2$ are shaded and assignments indicated schematically. Notice the absorbance scale change from spectrum a to the other two spectra. The stick diagram shows the calculated frequencies and intensities for $[CpRh(\mu\text{-}CO)]_2$, randomly enriched to 47% with ^{13}CO.

Table II. CO-Stretching Bands of $Cp_2Rh_2(CO)_3$ and $[CpRh(\mu\text{-}CO)]_2$ and Their ^{13}CO-Enriched Isotopomers in a $^{13}CO/N_2$ (1:10) Matrix[a]

complex	obsd	calcd	assignment[d]
		2000.5	$a(^{12}CO_t)_2(CO_b)$
	1986.0	1985.1	$b(^{12}CO_t)_2(CO_b)$
	1994	1994.1	$(^{12}CO_t)(^{13}CO_t)(CO_b)$
$Cp_2Rh_2(CO)_3$[b]	1947.2	1947.1	$(^{12}CO_t)(^{13}CO_t)(CO_b)$
		1955.9	$a(^{13}CO_t)_2(CO_b)$
	1940.0	1940.9	$b(^{13}CO_t)_2(CO_b)$
	1836.3	1836.3	$a(CO_t)_2(^{12}CO_b)$
	1795.3	1795.3	$a(CO_t)_2(^{13}CO_b)$
		1830.4	$a_g(^{12}CO_b)_2$
	1784.2	1783.5	$b_{1u}(^{12}CO_b)_2$
$[CpRh(\mu\text{-}CO)]_2$[c]	1817.5	1817.5	$a_1(^{12}CO_b)(^{13}CO_b)$
	1755.8	1756.1	$a_1(^{12}CO_b)(^{13}CO_b)$
		1789.6	$a_g(^{13}CO_b)_2$
	1743.3	1743.8	$b_{1u}(^{13}CO_b)_2$

[a] t, terminal; b, bridging; $\bar{\nu}$ (cm^{-1}). In this experiment, the bands of $CpRh(CO)_2$ and its isotopomers are also observed in positions close to those reported by Rest et al.[5] [b] C_2 symmetry, k_t = 1604, k_b = 1362, k_{tt} = 12 Nm^{-1}; k_{bt} assumed zero; rms error = 0.5 cm^{-1}. [c] D_{2h} symmetry, k_b = 1319, k_{bb} = 34 Nm^{-1}; rms error = 0.4 cm^{-1}. Double subscripts indicate an interaction force constrant. [d] Assignments are shown as an irreducible representation followed by the isotopomer. If no mass number is indicated, both ^{12}CO and ^{13}CO isotopomers contribute.

Anderson and Wrighton obtained no evidence for Rh–Rh bond fission of $Cp_2Rh_2(CO)_3$ in hydrocarbon glasses,[12] but we thought it worthwhile to explore this possibility in methane matrices. The expected products would be $CpRh(CO)_2$ and $CpRh(CO)(CH_3)H$, which absorbs at 2025 cm^{-1}.[3] In the event, the major product proved to be $[CpRh(\mu\text{-}CO)]_2$ with no formation of $CpRh(CO)_2$. Some very weak features grow in at 2030 and 2025 cm^{-1} on long-wavelength photolysis. However, they are probably associated with *cis*-$Cp_2Rh_2(CO)_3$, which is observed in the same region in all other matrices, and not with $CpRh(CO)(CH_3)H$.

Table III. Dichroic Ratios Measured in a Nitrogen Matrix

	$Cp_2Rh_2(CO)_3$		$[CpRh(\mu\text{-}CO)]_2$		
band, ν/cm^{-1}	1986	1844	1793	18500	30100[a]
$I_\parallel/I_\perp$[b]	1.18	1.22	0.93	1.03	1.07

[a] Overlap with band of $Cp_2Rh_2(CO)_3$. [b] Parallel and perpendicular are defined with respect to the polarization of the photolysis beam.

Polarized photolysis in matrices has been used for many years to make rigorous assignments and to distinguish different molecular structures.[16] The resulting dichroism has been used to demonstrate that $Mn_2(CO)_9$ has an η^1–η^2 bridging CO group,[17a] while $Cp^*_2Pt_2(\mu\text{-}CO)$ has a conventional bridging carbonyl.[17b] The method has also been used to study the mechanism of photoisomerization of $Fe_2(CO)_8$.[17c] Plane-polarized photolysis (λ > 280 nm, 90 min) of $Cp_2Rh_2(CO)_3$ in a N_2 matrix resulted in 30% conversion and in dichroism in the ν(CO) bands of the starting material and photoproduct. The dichroism of the two ν(CO) bands of the precursor was in the same direction, while that of the product carried the opposite polarization (Table III). Polarized UV/vis spectra, recorded in the region λ > 300 nm, could not be used to monitor dichroism in the starting material because of overlap with the product absorptions. However, slight positive dichroism ($I_\parallel/I_\perp$ > 1) was observed for the product band at 540 nm and the band at ~330 nm (product + precursor). The dichroism in the IR bands of the product provides convincing evidence that $[CpRh(\mu\text{-}CO)]_2$ contains conventional η^1–η^1 CO bridges like its Cp* analogue,[13] since otherwise dichroism would be negligible.[17] A full analysis of the dichroism and the assignment of the visible absorption are discussed later.

Photochemistry of $Cp_2Rh_2(CO)_3$ in Solution: Product Studies. The photochemical reactions of $Cp_2Rh_2(CO)_3$ with CO and C_2H_4 in hexane or heptane were examined by IR or NMR spectroscopy. Under 1 atm CO, rapid photochemical conversion (λ > 285 nm) to $CpRh(CO)_2$ ensued. With ethene as substrate (1 atm), a mixture of $CpRh(CO)_2$, $CpRh(CO)(C_2H_4)$, and $CpRh(C_2H_4)_2$ was formed (see Experimental Section).

Transient Photochemistry of $Cp_2Rh_2(CO)_3$ in Solution. Laser flash photolysis at 308 nm of $Cp_2Rh_2(CO)_3$ in cyclohexane ((0.5 – 1.0) × 10^{-4} mol dm^{-3}) under Ar or CO at room temperature yields a primary transient (rise time, <50 ns) whose visible spectrum (λ_{max} = 545 ± 5 nm) is almost identical with that of $[CpRh(\mu\text{-}CO)]_2$ characterized above (Figure 1b). This species is stable under Ar over the time scale available to us (up to 5 s), although recombination with CO does occur over a much slower time scale since subsequent UV and IR spectra show that the photolysis produces no net products. When the photolysis is carried out under an atmosphere of CO, the lifetime of $[CpRh(\mu\text{-}CO)]_2$ is found to be greatly reduced and inversely proportional to CO concentration (k_2 = (1.2 ± 0.1) × 10^3 dm^3 mol^{-1} s^{-1} at 292 K; Figure 3a,b, eq 1). In addition, by varying the temperature of

$$Cp_2Rh_2(CO)_3 \underset{CO,\,k_2}{\overset{h\nu}{\rightleftharpoons}} [CpRh(\mu\text{-}CO)]_2 \qquad (1)$$

the solution, the activation parameters, $\Delta H^\ddagger$ and $\Delta S^\ddagger$ have been found to be (22.3 ± 2.5) kJ mol^{-1} and (−110 ± 8) J mol^{-1} K^{-1}, respectively (Figure 3c). The negative value of $\Delta S^\ddagger$ is consistent with an associative mechanism, which is expected for a simple recombination reaction. In summary, these observations indicate simple ejection of CO from $Cp_2Rh_2(CO)_3$ upon photolysis to yield $[CpRh(\mu\text{-}CO)]_2$, with subsequent re-formation of starting complex via addition of CO.

When the photolysis of $Cp_2Rh_2(CO)_3$ in cyclohexane under CO (1.5 atm) is repeated with IR detection, we observe depletion of

(16) (a) Burdett, J. K.; Perutz, R. N.; Poliakoff, M.; Turner, J. J. *J. Chem. Soc., Chem. Commun.* **1975**, 157. (b) Burdett, J. K.; Grzybowski, J. M.; Perutz, R. N.; Poliakoff, M.; Turner, J. J.; Turner, R. F. *Inorg. Chem.* **1978**, *17*, 147. (c) Michl, J.; Thulstrup, E. W. *Acc. Chem. Res.* **1987**, *20*, 192, and references therein.

(17) (a) Dunkin, I. R.; Haerter, P.; Shields, C. J. *J. Am. Chem. Soc.* **1984**, *106*, 7248. (b) Dixon, A. J.; Firth, S.; Haynes, A.; Poliakoff, M.; Turner, J. J.; Boag, N. M. *J. Chem. Soc., Dalton Trans.* **1988**, 1501. (c) Fletcher, S. C.; Poliakoff, M.; Turner, J. J. *Inorg. Chem.* **1986**, *25*, 3597.

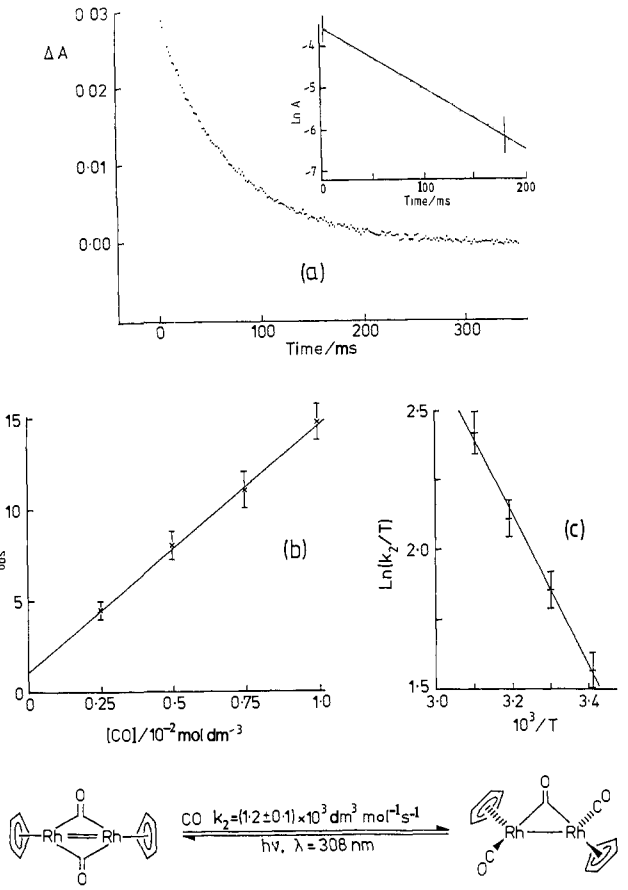

Figure 3. (a) Kinetic plot measured at 545 nm showing decay of $[CpRh(\mu\text{-}CO)]_2$ following laser photolysis of $Cp_2Rh_2(CO)_3$ in cyclohexane solution under 1 atm CO at 292 K. Inset shows first-order plot giving k_{obs}. (b) Graph showing variation of k_{obs} with CO concentration yielding second-order rate constant, k_2, for reaction of $[CpRh(\mu\text{-}CO)]_2$ with CO at 292 K. (c) Eyring plot showing variation of ln (k_2/T) with $1/T$, yielding activation parameters.

the starting material (ν(CO) = 1984, 1837 cm^{-1}) and formation of a product band at 1794 ± 2 cm^{-1}, which decays by first-order kinetics (k_{obs} = 17 s^{-1}). The position of this band, and the rate of decay, are fully consistent with the measurements obtained with UV/vis detection. The TRIR experiments did not provide evidence for the formation of $CpRh(CO)_2$ or $CpRh(CO)(C_6H_{11})H$ (see below), implying that Rh–Rh bond fission proceeds with a much lower quantum yield than CO loss on photolysis at 308 nm.

Laser Flash Photolysis of $CpRh(CO)_2$ and $CpRh(C_2H_4)CO$ with UV/vis Detection. In contrast to the UV/vis spectrum of $Cp_2Rh_2(CO)_3$, the spectra of $CpRh(CO)_2$ and $CpRh(C_2H_4)CO$ show only a single absorption band at 275 nm, with a tail extending into the visible resulting in a yellow color for these two complexes. Laser flash photolysis (λ = 308 nm) of $CpRh(CO)_2$ in cyclohexane or pentane (10^{-3}–10^{-2} mol dm^{-3}) under Ar yields a primary transient, A, detected at 360 nm with a rise time of ca. 400 ns. Since this is close to the limits of our instrument at this wavelength, we regard this as an upper limiting rise time. The spectrum of A shows no absorption maximum, but absorption declining over the range 340–400 nm. This species is stable for hundreds of microseconds, even in the presence of moderate concentrations of reactive ligands (e.g., CO, $P(OPh)_3$, Et_3SiH, and CH_4 at $\leq 10^{-2}$ mol dm^{-3}), and is formulated initially as CpRhCO or CpRh(CO)S, where S represents the solvent. Over a longer time period (ca. 100 ms), a second transient is observed to "grow in", which is assigned to $[CpRh(\mu\text{-}CO)]_2$ since it has the same visible absorption properties as this species in a matrix, and the same properties as the transient obtained following photolysis of $Cp_2Rh_2(CO)_3$ in solution (Figures 1b and 4a). The kinetics of formation of this dimer are not described by a second-order treatment on transient A, implying that this reaction does not proceed by simple dimerization. However, they may be analyzed by pseudo-first-order treatment. The final product of the laser photolysis in the absence of added ligands is $Cp_2Rh_2(CO)_3$, as shown by its characteristic IR and UV/vis spectra. Upon changing the solvent to benzene, the new primary transient (λ_{max} = 345 ± 5 nm) is observed to be much more stable than the transient in cyclohexane and no $[CpRh(\mu\text{-}CO)]_2$ is observed up to 5 s. Examination of the solution after a series of flashes shows that the final photoproduct is again $Cp_2Rh_2(CO)_3$, which is consistent with the product obtained under normal photochemical conditions.

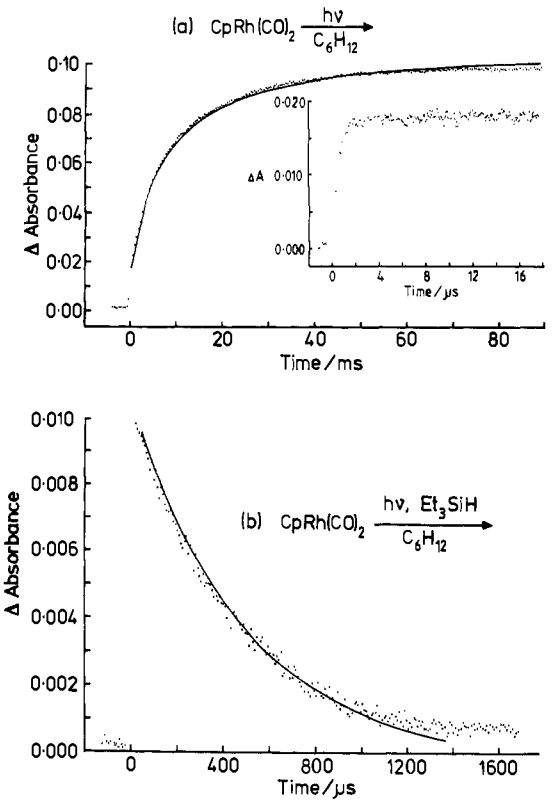

Figure 4. (a) Kinetic plot (dots) measured at 360 nm following laser photolysis of $CpRh(CO)_2$ in cyclohexane solution at room temperature under an argon atmosphere. Notice the initial rapid rise, followed by a slower rise. The initial rise is shown on a microsecond time scale in the inset. The simulated rise is shown as full line. The initial transient is A, the second slower transient is $[CpRh(\mu\text{-}CO)]_2$. (b) Kinetic plot measured at 360 nm following laser photolysis of $CpRh(CO)_2$ in cyclohexane containing 0.1 mol dm^{-3} Et_3SiH. Notice the expanded ordinate scale and the complete quenching of formation of $[CpRh(\mu\text{-}CO)]_2$. The full line shows the simulated decay. Simulation parameters for (a): [CpRh(CO)] (at time zero) = 10^{-4} mol dm^{-3}, k_1 = 9.0 × 10^5 dm^3 mol^{-1} s^{-1}, k_{-1} = 2.6 × 10^3 s^{-1}, k_3 = 1.3 × 10^{10} dm^3 mol^{-1} s^{-1}, $\epsilon([CpRh(\mu\text{-}CO)]_2)$ = 4400 dm^3 mol^{-1} cm^{-1} at 360 nm. Simulation parameters for (b) as above with k_2 = 2.6 × 10^8 dm^3 mol^{-1} s^{-1} and ϵ(CpRh(CO)S) = 100 dm^3 mol^{-1} cm^{-1} at 360 nm.

When the laser flash photolysis is carried out in C_6H_{12} but under an atmosphere of CO, the yield of $[CpRh(\mu\text{-}CO)]_2$ is found to be reduced by a factor of 4. In addition, the absorbance changes are consistent with partial re-formation of $CpRh(CO)_2$, implying that there is a competition for A between formation of $[CpRh(\mu\text{-}CO)]_2$ and back-reaction with CO under these conditions ([CO] = 1.1 × 10^{-2} mol dm^{-3}).[18] In order to quench out the formation of dinuclear products completely, a ligand has to be chosen whose concentration (or reactivity) can be made greater than that of CO at 1 atm. When $P(OPh)_3$ or Et_3SiH is used as substrate, at concentrations of ≥ 0.1 mol dm^{-3}, no transient absorption is observed at 545 nm, demonstrating the complete quenching of formation of $[CpRh(\mu\text{-}CO)]_2$. Triphenyl phosphite was chosen because it reacts thermally with $CpRh(CO)_2$ at the lowest rate

(18) Stephen, H., Stephen, T., Eds. *Solubilities of Inorganic and Organic Compounds*; Pergamon: Oxford, UK, 1963.

of all the phosphines and phosphites.[19] When the reaction is monitored at shorter wavelength, the decay of transient A can be observed (Figure 4b). However, when the concentration of ligand is changed under these conditions, the lifetime of the primary transient shows little dependence on changes in [L] (L = entering ligand; e.g., upon changing the concentration of Et_3SiH from 0.1 to 2.0 mol dm^{-3}, the lifetime of transient A is only reduced by a factor of 1.5). In the case of Et_3SiH, the limiting value for the rate of decay of transient A to generate $CpRh(CO)(SiEt_3)H$ is 2.7×10^3 s^{-1}.

Laser flash photolysis of $CpRh(C_2H_4)CO$ in C_6H_{12} (10^{-3} mol dm^{-3}) under Ar gives rise to absorption changes consistent with the formation of transient A by loss of C_2H_4. The initial increase in absorption (monitored at 360 nm) is followed by a further rise in absorption over several hundred milliseconds. The spectrum of this second transient corresponds to the dimer $[CpRh(\mu\text{-}CO)]_2$ and confirms the loss of C_2H_4 in the primary photochemical step. The presence of $CpRh(C_2H_4)S$ as an additional photoproduct is not so easy to verify since it has no unique absorption when compared with A. However, the ratio of the maximum absorbance of dimer to the initial absorbance at 360 nm is reduced substantially compared to that obtained under the same conditions following the photolysis of $CpRh(CO)_2$ and indicates the formation of $CpRh(C_2H_4)S$ as an additional species. ($CpRh(C_2H_4)S$ is known to absorb strongly at 360 nm from a previous study.[9] NMR studies of the initial photoproducts of $CpRh(CO)(C_2H_4)$ have indicated that the quantum yield for C_2H_4 loss exceeds that for CO loss.[3b]

The Nature of Transient A: UV Evidence for Solvent Participation. In a previous study we explored the transient photochemistry of $CpRh(C_2H_4)_2$ using laser flash photolysis with both UV/vis and IR detection.[9] Our observations showed that product formation (substitution of C_2H_4 by CO, cyclohexene, etc.) occurred either directly with the naked fragment or via reversible solvation of $CpRh(C_2H_4)$, where the $CpRh(C_2H_4)$–solvent interaction was found to be a specific one. These conclusions were based on two-stage product formation (determined by IR), the increased stability of $CpRh(C_2H_4)$ in C_6H_6 compared to C_6H_{12}, and the observation of saturation kinetics when monitoring the lifetime of the transient as a function of ligand concentration (UV/vis detection). The latter two points may also be applied to this current study to determine the nature of the primary transient, A. The increased stability of A in C_6H_6 as compared to C_6H_{12} indicates reaction with solvent to form either $CpRh(CO)(\eta^2\text{-}C_6H_6)$ or a phenyl hydride complex. In addition, the near invariance of the decay rate of A with ligand concentrations *in cyclohexane* solution, under conditions where no dimer formation occurs ([L] $\geq$ 0.1 mol dm^{-3}), indicates that the rate-limiting decay of A has been reached. These features can be accounted for by eq 2–4 where A is identified as a solvent complex, CpRh(CO)S, in both benzene and cyclohexane. In this formulation we do not distinguish between an alkane complex and an (alkyl) hydride or their arene/(aryl) hydride counterparts. The observation of A within the instrumental rise time implies that $k_1[S] \gtrsim$ (rise time)$^{-1}$ or $k_1 \gtrsim 3 \times 10^5$ dm^3 mol^{-1} s^{-1}. Kinetic saturation will be reached with $k_{obs} \simeq k_{-1}$ provided that $k_2[L] \gg k_1[S]$. The rate-limiting value for the decay of A corresponds to a value of $(2.7 \pm 0.3) \times 10^3$ s^{-1} for k_{-1}, the desolvation step.

$$CpRh(CO)_2 \xrightarrow{h\nu} CpRhCO \quad (2)$$

$$CpRhCO \underset{k_{-1},\,-S}{\overset{k_1,\,S}{\rightleftharpoons}} CpRh(CO)S \quad (A) \quad (3)$$

$$CpRhCO \xrightarrow[k_2,\,L]{} CpRh(CO)L \quad (4)$$

$$k_{obs} = \frac{k_2 k_{-1}[L]}{k_2[L] + k_1[S]}$$

$$[L]/k_{obs} = [L]/k_1 + k_1[S]/k_{-1}k_2$$

Extending this scheme to include the dimerization step, the kinetic data can be satisfied if this reaction proceeds via addition of CpRhCO to CpRh(CO)S with elimination of a solvent molecule. The overall scheme describing the photolysis of $CpRh(CO)_2$ in C_6H_{12} may therefore be obtained by combining eq 2–4 with eq 5 and 6:

$$CpRhCO + CpRh(CO)S \xrightarrow{k_3} [CpRh(\mu\text{-}CO)]_2 + S \quad (5)$$

$$[CpRh(\mu\text{-}CO)]_2 \xrightarrow{k_4,\,CO} Cp_2Rh_2(CO)_3 \quad (6)$$

This scheme is consistent with our observed kinetic and spectroscopic measurements and has been further tested by computer simulation (see Experimental Section). In particular, this modeling demonstrates that the formation of the dimer, $[CpRh(\mu\text{-}CO)]_2$, cannot arise by simple dimerization of CpRhCO or CpRh(CO)S. With the constraints on k_1 and k_{-1}, the simulation places k_3 at the diffusion-controlled limit of ca. 10^{10} dm^3 mol^{-1} s^{-1} for any reasonable value of the initial concentration of CpRhCO. On introduction of a ligand, L, into the analysis (eq 4), the quenching can be achieved with [L] $\geq$ 0.1 mol dm^{-3} if the value of $k_2 \sim 3 \times 10^8$ dm^3 mol^{-1} s^{-1}. With these parameters, the rate of decay of CpRh(CO)S agrees with experiment (L = Et_3SiH) and shows little variation with [L], implying that kinetic saturation has just been reached at this concentration of L. Simulated traces for the formation of $[CpRh(\mu\text{-}CO)]_2$ and for the decay of CpRh(CO)S are shown in Figure 4. The UV/vis work, therefore, allows the identification of the transient A as CpRh(CO)S, but does not distinguish between $CpRh(CO)(C_6H_{12})$ and $CpRh(CO)(C_6H_{11})H$.

Distinction between CpRh(CO)(alkane) and CpRh(CO)(alkyl) Hydride. In order to determine the exact nature of the primary transient A, $CpRh(CO)(C_6H_{12})$ or $CpRh(CO)(C_6H_{11})H$, we decided to carry out time-resolved IR experiments, as the ν(CO) mode of this transient would be expected to be much more sensitive to the oxidation state of the Rh center than any UV or visible absorption. The Ar matrix data[3,5] place ν(CO) for CpRhCO at 1968 cm^{-1}. Since the ν(CO) frequencies of $CpRh(CO)_2$ and $CpRh(C_2H_4)CO$ are shifted by 4–8 cm^{-1} to lower frequency in C_6H_{12} solution and in CH_4 matrices compared with their positions in Ar, a shift of at least this magnitude would be expected for the ν(CO) position of CpRhCO upon weak solvent coordination, giving us a predicted position for CpRh(CO)(alkane) of ca. 1960 cm^{-1}. In contrast $CpRh(CO)(CH_3)H$, obtained via photolysis of either $CpRh(CO)_2$ or $CpRh(C_2H_4)(CO)$ in CH_4 matrices, has a ν(CO) mode at 2025 cm^{-1}, consistent with a Rh(I) to Rh(III) oxidative addition.[3,5] It would be expected that an analogous species in solution (in this case a (cyclohexyl) hydride complex) would have a similar ν(CO) frequency and would therefore be readily distinguishable from a solvent complex.

Laser flash photolysis (λ = 308 nm) of $CpRh(CO)_2$ (2.5×10^{-3} mol dm^{-3}) under Ar results in a rapid (<10 μs) and permanent bleaching at 2050 and 1986 cm^{-1} due to partial loss of starting material. The instantaneous conversion of $CpRh(CO)_2$ amounts to $\lesssim$3%. This bleaching is accompanied by detection of a single product ν(CO) mode at 2018 $\pm$ 2 cm^{-1} (Figure 5a). This species, A, decays completely over ca. 100 ms by first-order kinetics (k_{obs} = 50 s^{-1}) with no reformation of $CpRh(CO)_2$. The formation of the secondary intermediate, $[CpRh(\mu\text{-}CO)]_2$, was not observed in this instance due to the small initial conversion and the moderate intensity of the bridging carbonyl mode for this intermediate. However, this experiment establishes that there is little, if any, formation of $Cp_2Rh_2(CO)_3$ via direct reaction between A and $CpRh(CO)_2$, since the two ν(CO) modes for this complex at 1981 and 1834 cm^{-1} are absent at all time scales up to 200 ms.

When the solution was placed under 1.5 atm CO ([CO] = 1.6×10^{-2} mol dm^{-3}),[18] the 2018-cm^{-1} band was observed again but with a lifetime reduced by a factor of ca. 10 (k_{obs} = 400 s^{-1}, Figure 5b). In addition, the decay of this transient is accompanied by re-formation of the bands of $CpRh(CO)_2$ to 80–90% of their original intensity. The reduction in lifetime of A under CO compared to Ar, together with the partial re-formation of $CpRh(CO)_2$ under CO, matches the postulated competition reaction for CpRh(CO) between CO addition and reaction with

(19) Schuster-Woldan, H. G.; Basolo, F. *J. Am. Chem. Soc.* **1966**, *88*, 1657.

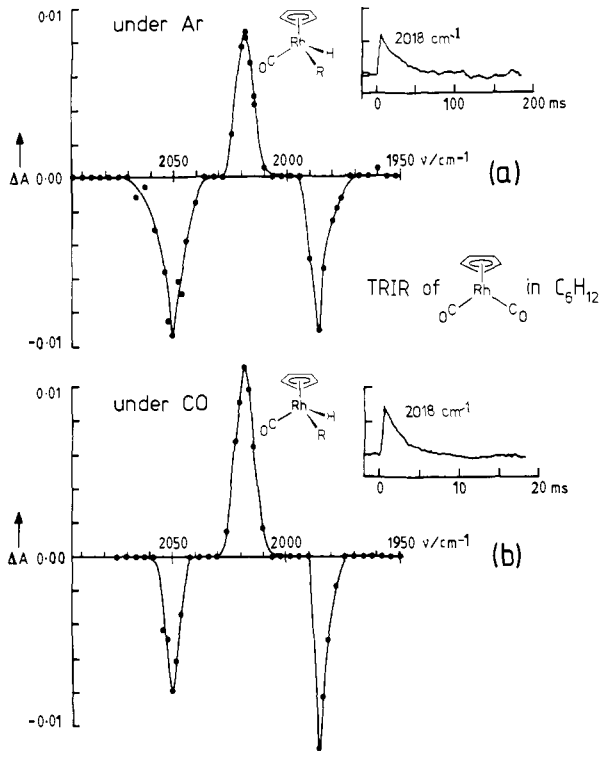

Figure 5. (a) Time-resolved infrared (TRIR) difference spectra obtained 20 ms following laser photolysis of $CpRh(CO)_2$ in cyclohexane solution under an argon atmosphere at room temperature. The negative peaks correspond to loss of starting material; the positive peak corresponds to gain of product A. The inset shows the kinetic plot for formation and decay of the product at 2018 cm^{-1}. (b) TRIR spectra measured 40 μs following laser photolysis of $CpRh(CO)_2$ under 1.5 atm CO. Notice the change in time scale for the kinetic plot compared to (a).

CpRh(CO)S shown earlier by use of flash photolysis with UV/vis detection. The position of the ν(CO) mode for A allows unambiguous assignment to the oxidative addition product $CpRh(CO)(C_6H_{11})H$. Other alternatives such as $(\eta^3\text{-}C_5H_5)Rh(CO)_2S$ may be excluded.

The increased photoreactivity of $CpRh(C_2H_4)CO$ compared with $CpRh(CO)_2$, both in solution and in matrices, led us to study this additional source of CpRhCO by time-resolved IR spectroscopy. Indeed, laser flash photolysis of $CpRh(C_2H_4)CO$ in C_6H_{12} (6.0×10^{-3} mol dm^{-3}) under Ar results in a loss of the parent ν(CO) mode at 1992 cm^{-1} together with gain of a product band at 2018 cm^{-1} with lifetime of ca. 15 ms (k_{obs} = 65 s^{-1}), assigned to the (cyclohexyl) hydride complex A observed previously (Figure 6a). On this occasion, the absorbance changes show a 2-fold increase both in loss of $CpRh(C_2H_4)CO$ and in formation of the oxidative addition product compared with the photolysis of $CpRh(CO)_2$. This increased yield enabled us to monitor both the decay of $CpRh(CO)(C_6H_{11})H$ at 2018 cm^{-1} and the consequent formation of the dinuclear intermediate, $[CpRh(\mu\text{-}CO)]_2$ at ~1786 cm^{-1} at the same rate (Figure 6a, inset). Upon moving to longer time scales (up to 1 s), the band due to the dinuclear complex at 1786 ± 4 cm^{-1} decays, and an increase in absorption at 1830 cm^{-1} ($Cp_2Rh_2(CO)_3$) is observed due to the reaction of $[CpRh(\mu\text{-}CO)]_2$ with CO. This reaction indicates that some of the starting material must have reacted via loss of CO. Considering the low concentration of CO, the decay of $[CpRh(\mu\text{-}CO)]_2$ is surprisingly fast. Unfortunately, the bridging region of the spectrum is complicated by the formation of additional products (formed within ca. 10 ms and therefore not formed directly from $CpRh(CO)(C_6H_{11})H$) with ν(CO) modes in the 1800–1820-cm^{-1} region.[20a] It is not clear as yet how the kinetic scheme is affected by the simultaneous presence of $CpRh(C_2H_4)$, CpRhCO, $CpRh(CO)(C_6H_{11})H$, CO, C_2H_4, and $CpRh(C_2H_4)CO$ in solution, but the details are being investigated further.

When the solution was placed under 1.5 atm CO, the decay of $CpRh(CO)(C_6H_{11})H$ was again found to increase by a factor of ca. 10 (k_{obs} = 500 s^{-1}, Figure 6b) and is accompanied by a recovery in the absorbance at ca. 1990 cm^{-1}. We deduce that $CpRh(CO)(C_6H_{11})H$ reacts to form $CpRh(CO)_2$ and/or $CpRh(CO)(C_2H_4)$—both of these molecules have peaks close to 1990 cm^{-1}.

Chart III. Transient Photochemistry of $CpRh(CO)_2$ and $Cp_2Rh_2(CO)_3$

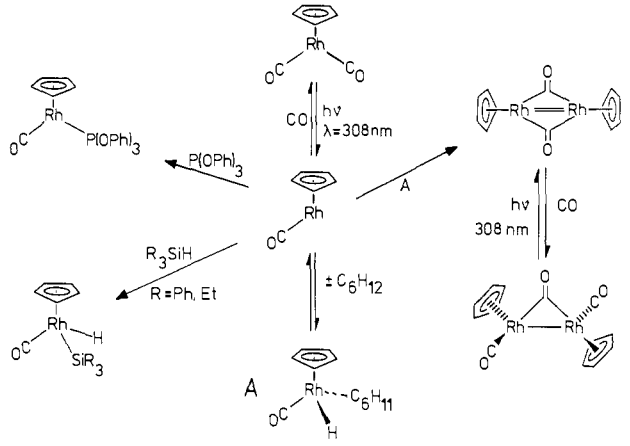

Chart IV. Possible Structures for the Core of $[CpRh(\mu\text{-}CO)]_2$

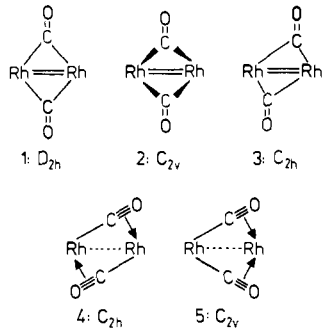

Discussion

This study has illustrated how laser flash photolysis with UV/vis and IR detection, in combination with matrix methods, can be used to provide detailed mechanistic information about organometallic photoreactions. Photolysis of $CpRh(CO)_2$ yields the coordinatively unsaturated complex CpRhCO (unobserved), which undergoes a rapid C–H activation of the solvent, C_6H_{12}, to give the Rh(III) species $CpRh(CO)(C_6H_{11})H$ characterized by time-resolved IR spectroscopy.[20b] The (cyclohexyl) hydride complex is extremely unstable and reacts with its reductive elimination product to give the dinuclear intermediate $[CpRh(\mu\text{-}CO)]_2$ (eq 5). The photolysis of $CpRh(CO)(C_2H_4)$ also leads, via $CpRh(CO)(C_6H_{11})H$, to $[CpRh(\mu\text{-}CO)]_2$. An alternative source of $[CpRh(\mu\text{-}CO)]_2$ is provided by the photolysis of $Cp_2Rh_2(CO)_3$. This reaction has been employed in solution via laser photolysis to yield activation parameters for recombination with CO, and via matrix isolation with polarized photolysis to yield information on the electronic and molecular structure of $[CpRh(\mu\text{-}CO)]_2$. The overall scheme for the transient photochemistry of $CpRh(CO)_2$ and $Cp_2Rh_2(CO)_3$ in solution is shown in Chart III.

Matrix and Polarized Photochemistry of $Cp_2Rh_2(CO)_3$. Like other dinuclear metal carbonyls,[22] $Cp_2Rh_2(CO)_3$ undergoes two

(20) (a) There is also a band at 1980–1990 cm^{-1} thought to be associated with these complexes, which overlaps that of $CpRh(C_2H_4)CO$. (b) At this stage we cannot distinguish between $CpRh(CO)(\eta^2\text{-}C_6H_6)$ and $CpRh(CO)(C_6H_5)H$ as products of photolysis of $CpRh(CO)_2$ in benzene.

(21) Meyer, T. J.; Caspar, T. V. *Chem. Rev.* **1985**, *85*, 187, and references therein.

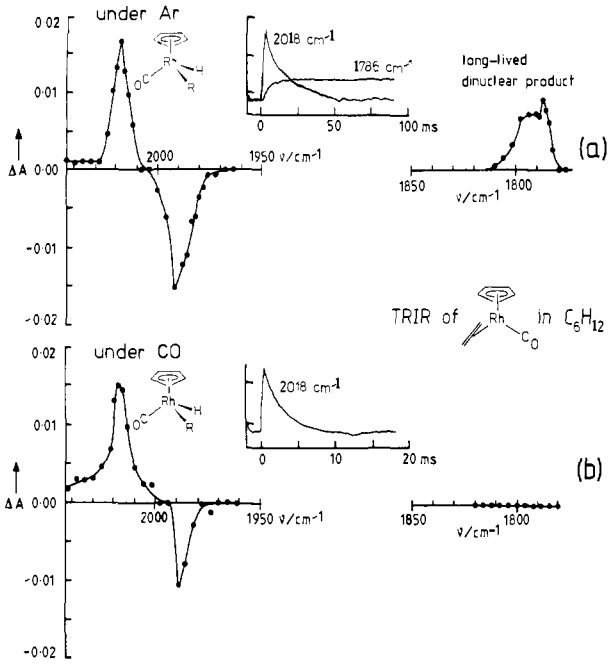

Figure 6. (a) TRIR difference spectra obtained 10 ms following laser photolysis of $CpRh(C_2H_4)CO$ in cyclohexane solution under an argon atmosphere at room temperature. Notice the high-frequency shift of the $\nu(CO)$ band at 2018 cm^{-1} and the production of dinuclear species. The inset shows the formation and decay of A at 2018 cm^{-1}, and the concurrent formation of $[CpRh(\mu\text{-}CO)]_2$ at 1786 cm^{-1}. (b) TRIR spectra obtained 2 ms following laser photolysis of $CpRh(C_2H_4)CO$ under 1.5 atm CO. Notice the absence of bands in the carbonyl bridging region.

different photochemical reactions. The major process in matrices is CO dissociation leading to $[CpRh(\mu\text{-}CO)]_2$, but the use of CO-doped matrices reveals the pathway to metal–metal bond cleavage and formation of $CpRh(CO)_2$. Of the five possible structures for the $Rh_2(CO)_2$ unit of $[CpRh(\mu\text{-}CO)]_2$ (**1**–**5**; Chart IV) structures **2** and **5** are incompatible with the IR data since they should show two bands for unlabeled $[CpRh(\mu\text{-}CO_2)]_2$ and four additional bands with full isotopic scrambling. However, structures **1**, **3**, and **4** are consistent with the observation of one band for $[CpRh(\mu\text{-}^{12}CO)]_2$ and four bands for the complete set of isotopomers. Further distinction can be achieved with the aid of polarized photolysis.

The key to understanding the polarized photolysis of $Cp_2Rh_2(CO)_3$ lies in the crystal structure of this molecule,[4a] which shows that it has C_2 symmetry with trans terminal CO groups and Cp rings. The angle made by the terminal (t) COs to the Rh–Rh axis is almost exactly 90° (88.2 (7)°), with the two terminal carbonyls and the Rh_2 unit close to coplanar. The bridging (b) CO lies in the perpendicular plane (C_b–Rh–C_t 91.9 (8)°) and bridges the COs symmetrically within experimental error.[4a] Polarized photolysis causes dichroic photodepletion, yielding a spectrum in which both $\nu(CO)$ bands of $Cp_2Rh_2(CO)_3$ carry similar dichroic ratios (Table III). There are two formally IR-active terminal $\nu(CO)$ modes ($a + b$). However, as a consequence of the molecular structure, the symmetric terminal mode can only acquire intensity by mixing with other a modes at considerably lower frequency (e.g., the bridging mode) and is expected to be extremely weak. It is not observed. Thus, the observed $\nu(CO)_t$ mode has b symmetry and a transition moment parallel to y, while the $\nu(CO)_b$ mode has a symmetry and a transition moment parallel to z (see Charts V and VI). The two modes can only carry the same dichroic ratios if they are both perpendicular to the photoactive transition, which must therefore lie along the Rh–Rh axis, x. (The photoactive transition may well correspond to the lowest energy absorption at ~428 nm, but it is too weak to record any dichroism.)

Chart V. Polarized Photolysis of $Cp_2Rh_2(CO)_3$

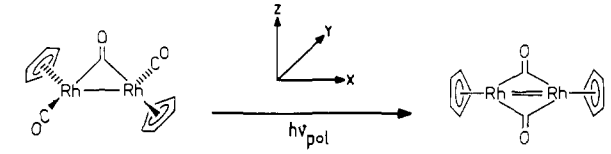

Dichroic Photodepletion	Dichroic Photoproduction
Infrared	Infrared
C_2 $\nu(CO)_t$ = o (①) + b (②)	D_{2h} $\nu(CO)_b$ = a_g (①) + b_{1u} (②)
$\nu(CO)_b$ = a (③)	
Mode 1: not observed	Mode 1: inactive
Mode 2: y t.m.	Mode 2: z t.m.
Mode 3: z t.m.	
UV/vis	UV/vis
Photoactive transition	540 nm: x t.m.
x t.m.	330 nm: x t.m.
x depleted	x enhanced
y, z enhanced	y, z depleted

t.m. = transition moment

Chart VI. Polarized Photolysis of $Cp_2Rh_2(CO)_3$

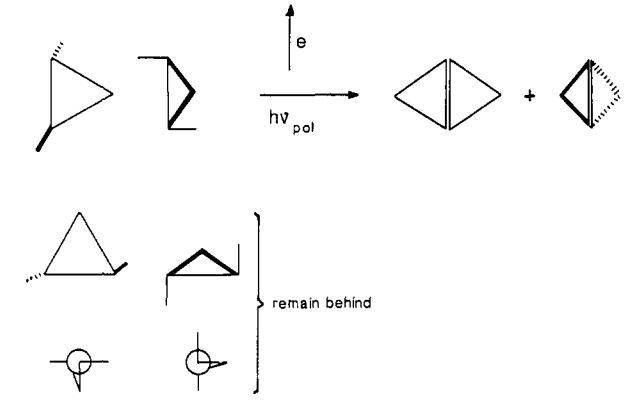

Since $Cp_2Rh_2(CO)_3$ is preferentially depleted when its x axis lies parallel to the direction of the electric vector employed for photolysis, we expect that the photoproduct, $[CpRh(\mu\text{-}CO)]_2$, will be formed preferentially with its Rh–Rh axis lying in the same direction. Assuming it has structure **1** with D_{2h} local symmetry, it should have two bridging $\nu(CO)$ modes; the symmetric stretch (a_g) is IR-inactive, while the antisymmetric stretch (b_{1u}) is observed. Defining the axes as for $Cp_2Rh_2(CO)_3$, the IR-active mode has its transition moment along z. When the transition moments for the starting material and products are parallel to one another, their dichroic ratios should be opposite. Chart V summarizes the directions of the transition moments and the expected dichroism of the spectra. (Notice that the terms *depleted* and *enhanced* are not intended to indicate any photoreorientation.) Chart VI shows the effect of polarized photolysis with the electric vector of the photolysis beam parallel to the laboratory Y axis on three extreme sets of orientations of $Cp_2Rh_2(CO)_3$. The dichroic ratio for the $\nu(CO)$ band of $[CpRh(\mu\text{-}CO)]_2$ is found to be <1, as predicted by this argument.

If in contrast, structure **4** applied (C_{2h}), there would again be one IR-active CO-stretching mode (b_u) but its transition moment would lie at ~45° to the Rh–Rh axis, giving no net polarization.[17]

(22) (a) Cirjak, L. M.; Ginsberg, R. E.; Dahl, L. F. *Inorg. Chem.* **1982**, *21*, 940. (b) Pinhas, A. R.; Albright, T. A.; Hofmann, P.; Hoffmann, R. *Helv. Chim. Acta* **1980**, *63*, 29.

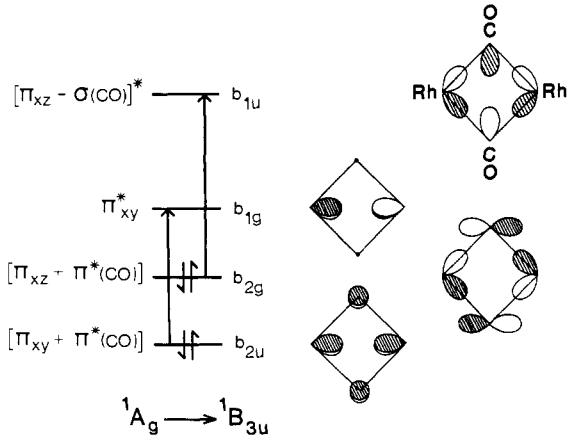

Figure 7. One-electron MO diagram for $[CpRh(\mu\text{-}CO)]_2$ assuming D_{2h} local symmetry. The two allowed transitions shown with arrows, both $^1A_g \rightarrow {}^1B_{3u}$, have transition moments along the Rh=Rh bond (x) and are expected to be strongly mixed. The form of the orbitals and their order is adapted from ref 22a, but our assignment differs from this reference.

The final structure remaining is **3**, which also has C_{2h} local symmetry, but retains the bridging carbonyl groups, perpendicular to the Rh–Rh axis. This structure cannot be excluded rigorously. Thus, the polarization and isotopic experiments establish that $[CpRh(\mu\text{-}CO)]_2$ has trans-planar CO-bridges as in structures **1** and **3**, with the carbonyl vectors perpendicular to the Rh–Rh axis. The structure of the Cp* analogue corresponds to **1**.[13]

The electronic structures of $[CpCo(\mu\text{-}CO)]_2$ and $[Cp^*M(\mu\text{-}CO)]_2$ (M = Co, Rh, Ir) have been investigated extensively.[22,23] These studies and the calculations[22b] on $[CpRh(\mu\text{-}CO)]_2$ yield the pattern of frontier orbitals shown in Figure 7 (the axes have been defined as in Chart V rather than as in ref 22). If we retain D_{2h} local symmetry, there are two allowed electronic transitions, which both have B_{3u} upper states and transition moments parallel to x, the Rh–Rh bond. We therefore predict that they should exhibit dichroic ratios of >1, as is observed for the product bands at 540 and 330 nm. We conclude that these bands correspond to the pair of $^1A_g \rightarrow {}^1B_{3u}$ transitions of the $Rh_2(\mu\text{-}CO)_2$ π-bonding unit.[24] This argument is unaffected by the move to structure **3**, with C_{2h} symmetry.

Reaction Kinetics. The transient photochemistry of $CpRh(CO)_2$, $CpRh(C_2H_4)CO$, and $Cp_2Rh_2(CO)_3$ reveals two major surprises: (i) the first observed product from $CpRh(CO)_2$ and $CpRh(C_2H_4)CO$ is $CpRh(CO)(C_6H_{11})H$ and all carbonyl photoproducts appear to be formed via this C–H activation product; (ii) the dinuclear product observed from $CpRh(CO)_2$ is $[CpRh(\mu\text{-}CO)]_2$ and not $Cp_2Rh_2(CO)_3$.

The kinetics of formation of dinuclear complexes from mononuclear fragments have been studied before, but it is more usual for the formation of dinuclear species to occur via reaction with the precursor complexes (e.g., CpCoCO with $CpCo(CO)_2$,[7b] $CpMn(CO)_2$ with $CpMn(CO)_3$,[25] Cp_2Mo with Cp_2MoH_2,[26] and $Cr(CO)_5$ with $Cr(CO)_6$[27]) than to observe reaction between two unstable complexes. An analogy between the reaction of $CpRh(CO)(R)H$ with CpRhCO may be drawn with the reaction following photolysis of $Cp^*Re(CO)_3$ in benzene.[28] In the latter case, the η^2-benzene complex resulting from CO loss and arene coordination undergoes a dimerization process with overall loss of one benzene molecule:

$$2Cp^*Re(CO)_2(\eta^2\text{-}C_6H_6) \rightarrow [Cp^*Re(CO)_2]_2(\mu\text{-}\eta^2,\eta^{2\prime}\text{-}C_6H_6) + C_6H_6$$

Since the η^2-arene complex is only moderately stable, yielding $Cp^*_2Re_2(CO)_5$ as an additional dinuclear product, it seems likely that benzene coordination is reversible, allowing attack on this complex by the naked fragment $Cp^*Re(CO)_2$. The reason that the (fragment + precursor) pathway is usually preferred to dimerization of the reaction intermediate probably lies in the higher concentration of the precursor complexes compared with those of the reaction intermediate. In our system CpRhCO must be more highly reactive toward $CpRh(CO)(R)H$ than toward $CpRh(CO)_2$.

When reactive ligands are added to the solution, competition for CpRhCO is observed between dimerization and ligand attack. Since the dimerization reaction proceeds via reaction of CpRhCO with $CpRh(CO)(C_6H_{11})H$ with a rate constant close to the diffusion limit, it is necessary to have a high concentration of ligand ($[L] \geq 0.1$ mol dm^{-3}) to completely quench the dimerization. The reversible C–H activation of C_6H_{12} by CpRhCO has been further verified by the observation of saturation kinetics[9] with Et_3SiH as the trap for the naked fragment. From these data, k_{-1}, the rate of reductive elimination of C_6H_{12} from $CpRh(CO)(C_6H_{11})H$ is determined to be $(2.7 \pm 0.3) \times 10^3$ s^{-1}, while the ratio k_2/k_1 is 15 (see eq 2 and 3). Since the k_2/k_1 ratio shows a marked preference for oxidative addition of Si–H in Et_3SiH compared with C–H insertion of C_6H_{12}, we expect that the two-stage product formation indicated by the scheme should be significantly affected by the concentrations of Et_3SiH ($[Et_3SiH]$ = 0.1–2.0 mol dm^{-3}, $[C_6H_{12}]$ = 9.3 mol dm^{-3}). More quantitatively, the yield of $CpRh(CO)(C_6H_{11})H$ formed initially should show an inverse relationship to the concentration of Et_3SiH used in each experiment. However, such an effect is not observed. In addition, when $P(OPh)_3$ is used as a trap for CpRhCO, quenching of the dimerization step is observed with $[P(OPh)_3] > 0.1$ mol dm^{-3}, but the value of k_{obs} for the decay of $CpRh(CO)(C_6H_{11})H$ is significantly lower compared with that obtained when using Et_3SiH at the same concentration ($[P(OPh)_3] = [Et_3SiH] = 0.1$ mol dm^{-3}, $k(P(OPh)_3) = 5.0 \times 10^1$ s^{-1}, $k(Et_3SiH) = 2.0 \times 10^3$ s^{-1}). Nevertheless, $P(OPh)_3$ competes with the dimerization step (eq 5) under these conditions. One possible explanation for both of these observations is that CpRhCO inserts into the C–H bonds of the alkyl and aryl groups of Et_3SiH and $P(OPh)_3$, respectively, to yield kinetically unstable products. The increased lifetime of CpRhCO in the presence of arene C–H bonds has already been observed following photolysis of $CpRh(CO)_2$ in C_6H_6 and may explain the increase in apparent stability of the transient in C_6H_{12} in the presence of $P(OPh)_3$. The reactions with ligands and the effect of arene solvents will be examined in more detail in future TRIR experiments.

Conclusions

The primary product of photolysis of $CpRh(CO)_2$ in cyclohexane is $CpRh(CO)(C_6H_{11})H$ formed by insertion of CpRhCO into solvent C–H bonds within 400 ns.[29] The same complex is formed as one of the photoproducts of $CpRh(CO)(C_2H_4)$. The formation of this (alkyl) hydride complex is kinetically favorable, but it reacts within milliseconds to form more stable products. In the absence of other substrates, it forms the dinuclear, purple, $[CpRh(\mu\text{-}CO)]_2$, which itself is unstable with respect to red $Cp_2Rh_2(CO)_3$. The kinetics of reaction, including activation parameters, for the process $[CpRh(\mu\text{-}CO)]_2 + CO$, have been measured by independent laser flash photolysis of $Cp_2Rh_2(CO)_3$. In the presence of high concentrations of other ligands, the (alkyl)

(23) Griewe, G. L.; Hall, M. B. *Organometallics* **1988**, *7*, 1923.
(24) The lowest energy absorption of $[Cp^*Co(\mu\text{-}CO)]_2$ was previously assigned to the HOMO–LUMO transition.[22a] However, considering the effective center of symmetry and the high extinction coefficient, we prefer to assign it as shown for the CpRh analogue in Chart VI.
(25) Creaven, B. S.; Dixon, A. J.; Kelly, J. M.; Long, C.; Poliakoff, M. *Organometallics* **1987**, *6*, 2600.
(26) Perutz, R. N.; Scaiano, J. C. *J. Chem. Soc., Chem. Commun.* **1984**, 457.
(27) Kelly, J. M.; Long, C.; Bonneau, R. *J. Phys. Chem.* **1983**, *87*, 3344.
(28) (a) Van der Heijden, H.; Orpen, A. G.; Pasman, P. *J. Chem. Soc., Chem. Commun.* **1985**, 1576. (b) A reviewer has also drawn our attention to the analogy with binuclear reductive elimination reactions; see, e.g.: Nappa, M. J.; Santi, R.; Halpern, J. *Organometallics* **1985**, *4*, 34.
(29) A similar oxidative addition of cyclohexane has also been observed by photolysis of $Cp^*Rh(CO)_2$ in liquid krypton doped with cyclohexane (Weiller, B. H.; Wasserman, E. P.; Bergman, R. G.; Moore, C. B.; Pimentel, G. C., submitted for publication). We are grateful to Prof. Bergman for disclosing these results prior to publication.

hydride complex decays via saturation kinetics to form conventional products such as $CpRh(CO)(SiEt_3)H$ and $CpRh(CO)[P(OPh)_3]$. These results carry the implication that other, apparently "innocent", reactions of organometallics may proceed via short-lived C–H activation products. These conclusions depend on the combined use of information from time-resolved UV and IR experiments with matrix isolation data involving both UV and IR detection. The TRIR measurements cover both bridging and terminal ν(CO) regions. Polarized photolysis of $Cp_2Rh_2(CO)_3$ in matrices generates partially oriented $[CpRh(\mu\text{-}CO)]_2$. The dichroic spectra and isotopic data have been used to demonstrate that the $Rh_2(\mu\text{-}CO)_2$ unit is planar with the bridging carbonyls oriented perpendicular to the metal–metal bond, and that the lowest energy electronic transition is polarized along the Rh–Rh axis. In CO matrices and CO-saturated solutions, Rh–Rh bond fission competes with CO loss from $Cp_2Rh_2(CO)_3$. The absence of $CpRh(CO)_2$ in the TRIR experiments on $Cp_2Rh_2(CO)_3$ implies a lower quantum yield at 308 nm for Rh–Rh bond fission than CO loss. The current time-resolved data are fully consistent with the prior matrix studies of $CpRh(CO)_2$ and $CpRh(CO)(C_2H_4)$ and the present study of $Cp_2Rh_2(CO)_3$.

Experimental Section

Apparatus. The apparatus at York for flash photolysis with UV detection consists of an excimer laser (Lambda Physik EMG-50) operating at 308 nm (XeCl) as the exciting source, coupled to an Applied Photophysics laser kinetic spectrometer with a Xe arc lamp (which can be pulsed for microsecond time scales) as a white light source. The laser pulse (ca. 20 ns) is focused into a beam of ca. 1-mm diameter and directed through the sample together with the monitoring beam in the collinear arrangement by means of a quartz beam splitter. The excitation can also be attenuated by means of neutral density filters in order to reduce shock waves in the solution. Light falling on the photomultiplier detector is sampled by a Gould Biomation 4500 digital oscilloscope and transferred to an Apple IIe microcomputer for data analysis and storage. Transient decays are usually analyzed as 16 shot averages to increase the signal to noise ratio and improve kinetic analysis. In addition, the Apple is used to fire the laser and synchronize the timing of the monitoring beam. Using this facility, we are able to operate the laser and arc lamp independently, and also obtain pre- and postexcitation absorption profiles in a singlet shot. Triggering of the oscilloscope is achieved by diverting part of the laser beam and focusing onto a photodiode. Transient spectra are obtained by the point by point method and correspond to difference spectra after particular fixed times following the laser flash. The sample was maintained at room temperature unless stated otherwise.

The principles of the apparatus at Mülheim for time-resolved infrared spectroscopy (TRIR) have been described previously.[14c,30] The 308-nm flash was generated by an excimer laser (Lambda Physik EM200). A globar, which served as the IR source, was focused by two CaF_2 lenses, first onto the standard IR flow cell and then onto the entrance slit of a modified Spex double monochromator (2–8-cm^{-1} resolution, depending on choice of slit width). The detection equipment and computer-assisted data evaluation are described in ref 14c. The IR cell, maintained at room temperature, is connected to a reservoir containing stock solution of the complex under 1.5 atm pressure of either CO or Ar. A 0.7-cm^3 portion of stock solution is allowed into the cell via a magnetic valve for each shot, so allowing TRIR kinetic traces to be collected point by point from a fresh solution.

A description of the York apparatus for matrix isolation is given elsewhere.[3] Matrix IR spectra were recorded on a Perkin-Elmer 580 spectrometer fitted with a common-beam polarizer or on a Mattson Sirius interferometer at 1-cm^{-1} resolution. The mercury arc (Philips HPK 125 W with water filter) and the UV spectrometer were polarized with the aid of an Oriel UV polarizer. $Cp_2Rh_2(CO)_3$ was deposited by continuous spray-on from a sidearm heated to 338–340 K onto a window cooled to 20 K.

Materials. $CpRh(C_2H_4)CO$[3a] and $Cp_2Rh_2(CO)_3$[4b] were synthesized by standard methods. $CpRh(CO)_2$ was made by reaction of $[Rh(CO)_2Cl]_2$ with TlCp in Et_2O[31] and purified by trap to trap distillation. Cyclohexane and benzene (Aldrich, Gold Label grade) were dried over sodium and distilled prior to use. Rhodium trichloride was the gift of BP Chemicals. CO (BOC research grade), ^{13}CO (Amersham, nominally 99 atom % but contained ca. 11% $^{13}C^{18}O$), Et_3SiH (Fluka), TlCp (Aldrich), and $P(OPh)_3$ (Aldrich) were used as received. All solutions for flash photolysis with UV detection were degassed in quartz cuvettes (pathlength, 10, 2, or 1 mm) fitted with a PTFE stopcock and a degassing bulb, by using the freeze–pump–thaw technique at 10^{-4} Torr, and back-filled with CO or Ar to 1 atm.

Photolysis of $Cp_2Rh_2(CO)_3$ in Solution. (a) Under CO. $Cp_2Rh_2(CO)_3$ (3 mg, 7×10^{-6} mol) was dissolved in 5 cm^3 of heptane and photolyzed under 1 atm CO at 298 K in a Pyrex ampule ($\lambda > 285$ nm) for 2 h. The solution turned from red to yellow. The product was identified by IR spectroscopy as $CpRh(CO)_2$. **(b) Under C_2H_4.** $Cp_2Rh_2(CO)_3$ (8 mg, 2×10^{-5} mol) was dissolved in 3 cm^3 of hexane and photolyzed under 1 atm C_2H_4 for 8 h as above. After removal of the solvent, the residue was redissolved in CD_2Cl_2. The products $CpRh(CO)_2$, $CpRh(CO)(C_2H_4)$, and $CpRh(C_2H_4)_2$ were identified by ^1H NMR spectroscopy.

Analysis of Kinetic and Spectroscopic Data. Kinetics were simulated with a modified version of a program developed by Shell Research: SIMULA.[32] The input for this program begins by defining the reaction scheme and the period of simulation. The concentrations of the reagents and the forward and reverse rate constants for each elementary step must also be entered. The output consists of a concentration versus time plot in graphical or numerical format. The input parameters are refined manually. For example, the reaction of $CpRh(CO)_2$ with Et_3SiH was simulated by using the following ranges of parameters: $[CpRh(CO)]$ (at time zero) = 10^{-5}–10^{-4} mol dm^{-3}, $[Et_3SiH]$ = 0.2–2.0 mol dm^{-3}, k_1 = 10^5–10^7 dm^3 mol^{-1} s^{-1}, k_{-1} = 10^3–10^4 s^{-1}, k_2 = 10^7–10^9 dm^3 mol^{-1} s^{-1}, k_3 = 10^9–10^{11} dm^3 mol^{-1} s^{-1}.

The effects of isotopic labeling on IR spectra of metal carbonyls including frequency and intensity distribution (see Figure 2) were simulated by standard methods.[33]

Acknowledgment. We are pleased to acknowledge the support of SERC, the EEC, The Royal Society, British Gas, and BP Chemicals. We are particularly grateful to Prof. J. J. Turner for his advice and to Prof. K. Schaffner for his encouragement and guidance and to Miss K. Fuchs for technical assistance.

(30) (a) Hermann, H.; Grevels, F.-W.; Henne, A.; Schaffner, K. *J. Phys. Chem.* **1982**, *86*, 5151. (b) Church, S. P.; Grevels, F.-W.; Hermann, H.; Schaffner, K. *Inorg. Chem.* **1985**, *24*, 418.

(31) McCleverty, J. A.; Wilkinson, G. *Inorg. Synth.* **1966**, *8*, 211.

(32) Salman, T. M. F. D.Phil. Thesis, University of York, 1984. Prothero, A. A computer program for solving stiff chemical rate equations. Shell Research TRCP 1657 (a), 1970.

(33) Perutz, R. N.; Turner, J. J. *Inorg. Chem.* **1975**, *14*, 262.